Research article

# Synthesis and characterization of a 2-periodic cadmium-based metal-organic framework: A study on reversible water adsorption☆

Nabanita Chatterjee [a], Marcello Mutti [a,b], Paolo Pelagatti [b], Clive L. Oliver [a,*]

[a] *Department of Chemistry, University of Cape Town, Rondebosch, Cape Town, South Africa*
[b] *Dipartimento di Scienze Chimiche, della Vita e della Sostenibilità Ambientale, Università di Parma, Parco Area delle Scienze 17/A, 43124 Parma, Italy*

## GRAPHICAL ABSTRACT
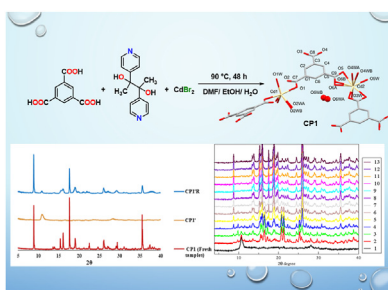


## ARTICLE INFO

## ABSTRACT

A previously-reported cadmium-based two-periodic metal-organic framework $[Cd_{1.5}(BTC)(H_2O)_{4.5}]_n \cdot n H_2O$ (**CP1**) has been re-synthesized, where $H_3BTC$ = 1,3,5-benzenetricarboxylic acid. **CP1** was characterized with single crystal X-ray diffraction (SCXRD), powder X-ray diffraction (PXRD) followed by various thermal analyses such as thermogravimetric analysis (TGA), hot stage microscopy (HSM) and differential scanning calorimetry (DSC). **CP1** is composed of 2-periodic layers, which are interdigitated. Heating can effectively remove the uncoordinated and coordinated water molecules resulting in an amorphous product **CP1′**. The original framework can be regenerated by readsorption of water from the atmosphere, indicating that the dehydration is reversible.

## 1. Introduction

The design and synthesis of metal-organic frameworks (MOFs) have been extensively studied due to the attraction of their adjustable, structure-dependent properties which can be utilized in various applications such as gas sorption, catalysis, luminescence and molecular recognition [1, 2, 3]. The frameworks of MOFs, which fall in the category of coordination polymers, are constructed from metal ions that act as 'nodes' and organic bridging ligands that act as 'spacers' [4]. Water

stability of these MOFs still remain an important challenge, as various industrial environments, where these materials may find applications, have atmospheric water present [5]. One such example, may be the removal of $CO_2$ from flue gas mixtures ($CO_2/N_2$ = 85/15) which have a water-rich environment. In case the primary MOF for this purpose is not water-stable, a secondary MOF can be used to remove water from the atmosphere. In this work, the MOF $[Cd_{1.5}(BTC)(H_2O)_{4.5}]_n \cdot n H_2O$ (**CP1**) ($H_3BTC$ = 1,3,5-benzenetricarboxylic acid) was synthesized by a hydrothermal method. The structure was first reported by Michaelides and
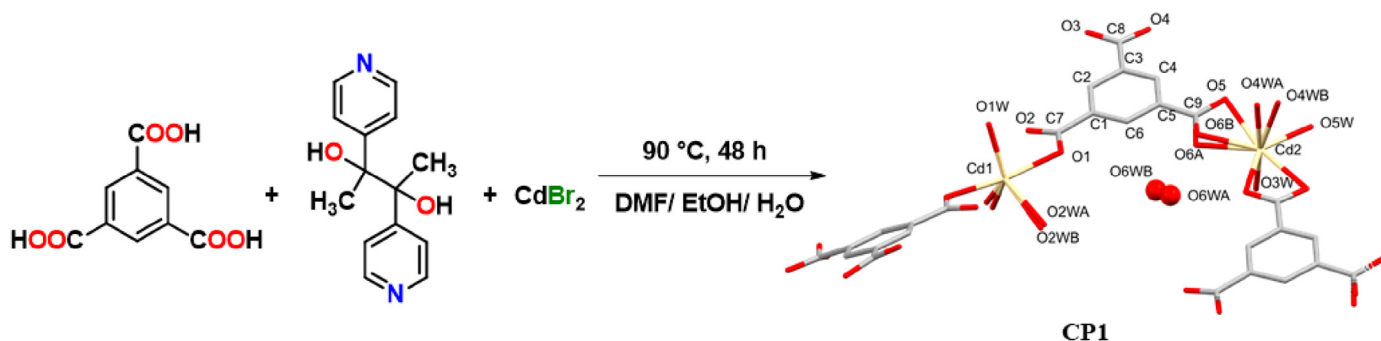
**Scheme 1.** Synthesis of **CP1**.

Skoulika et al., and subsequently by Wu et al. (both at 293 K) as part of a fluorescence study [6, 7]. The current work adds to the studies on this MOF by reporting on the single crystal structure at 100 K and assessing the hydrogen bonding that involves coordinated and uncoordinated water molecules. In addition, the dehydration and rehydration properties of the MOF using infrared (IR), hot stage microscopy (HSM), thermogravimetric analysis (TGA) and differential scanning calorimetry (DSC), as well as *in situ* powder X-ray diffraction (PXRD) were assessed. The MOF's dehydration and subsequent loss of crystalline structure is reversible in the presence of water vapour, showing that the dehydrated MOF could possibly be used as a water 'scavenger' in applications where dry environments are required.

## 2. Materials and methods

### 2.1. Materials and instrumentation

All reagents and solvents were commercially available and used as received. 1,3,5-Benzenetricarboxylic acid ($H_3BDC$), 2,3-di(4-pyridyl)-2,3-butanediol and $CdBr_2 \cdot 4H_2O$ were purchased from Sigma Aldrich. Solvents were not dried and may have contained some water. Thermogravimetric analysis (TGA) and differential scanning calorimetry (DSC) were performed using a TA Instruments TGA Q500 and a DSC Q200, respectively, with samples heated at a heating rate of 10 °C min$^{-1}$ in the temperature range 20–600 °C and 20–400 °C for TGA and DSC, respectively, under a dry nitrogen flow of 60 mL min$^{-1}$. Approximately 2–5 mg of sample was placed in an open crucible for each analysis, except for dehydration and rehydration studies where sample masses were ~10 mg. Fourier-transform infrared (FT-IR) spectroscopy was performed in the range 4000–500 cm$^{-1}$ on a PerkinElmer Spectrum Two FT-IR spectrometer using attenuated total reflectance (ATR). Hot stage microscopy (HSM) was performed using a Linkam THMS600 hot stage and Linkam TP92 control unit fitted to a Nikon SMZ-10 stereoscopic microscope. Crystals were placed on a cover slip under silicon oil to visualize solvent release using HSM. Images of thermal events were monitored with a Sony Digital Hyper HAD colour video camera and visualized on the Soft Imaging System program analySIS. Powder X-ray diffraction (PXRD) measurements were performed on a Bruker D8 Advance X-ray diffractometer in the 4–40° 2θ range using a 0.02° s$^{-1}$ step size rate and X-rays generated at 30 kV and 40 mA. Experimentally-obtained PXRD patterns were compared to the simulated PXRD patterns calculated from the single crystal structure coordinates using MERCURY [8].

### 2.2. Synthesis and crystallization: preparation of [Cd$_{1.5}$(BTC) (H$_2$O)$_{4.5}$]$_n$·nH$_2$O (CP1)

Benzene-1,3,5-tricarboxylic acid (13 mg, 0.06 mmol) and 2,3-di(4-pyridyl)-2,3-butanediol (15 mg, 0.06 mmol) were dissolved together with cadmium bromide (49 mg, 0.14 mmol) in 3 mL *N,N'*-dimethylformamide (DMF), 2 mL water and 1 mL ethanol (EtOH) with continuous stirring. The mixture was heated in an oven at 90 °C for 48 h

(Scheme 1). Flat, colourless crystals of **CP1** were obtained upon slow cooling of the solution at a rate of 10 °C h$^{-1}$. Interestingly, the pyridyl-based co-ligand was not present in the structure of **CP1**. Subsequently, the synthesis was attempted without its presence, however, in these cases, **CP1** was co-crystallized with presence of other by-products, thus the presence of 2,3-di(4-pyridyl)-2,3-butanediol was retained for future preparations, even though it was not part of the crystallized product.

### 2.3. Single crystal X-ray diffraction studies

A single crystal of suitable quality was selected and mounted using cryoloop in Paratone N oil. Data collections were carried out on Bruker DUO APEX II CCD diffractometer using graphite monochromated Mo Kα (λ = 0.71073 Å) radiation, generated at 50 kV and 30 mA, with the crystal cooled to 100 K using an Oxford Cryostream-700. Data reduction and unit cell refinement were performed using SAINT-Plus [9]. All intensity data were scaled and corrected for Lorentz-polarisation and absorption effects using SADABS [10]. Structure solution and refinement were implemented using the crystallographic suite OLEX2 [11]. The crystal structures were solved by SHELXT, with subsequent refinement

**Table 1.** Crystal data and refinement parameters of **CP1**.

| | |
|---|---|
| Empirical formula | $C_9H_{14}Cd_{1.5}O_{11.5}$ |
| Formula weight | 474.80 |
| Temperature/K | 100.0 |
| Crystal system | Monoclinic |
| Space group | *C2/c* |
| a/Å | 19.0101 (16) |
| b/Å | 7.3447 (7) |
| c/Å | 20.4158 (17) |
| α/° | 90 |
| β/° | 97.281 (2) |
| γ/° | 90 |
| Volume/Å$^3$ | 2827.5 (4) |
| Z | 8 |
| ρ$_{calc}$/g cm$^{-3}$ | 2.231 |
| μ/mm$^{-1}$ | 2.336 |
| F(000) | 1856.0 |
| Crystal size/mm$^3$ | 0.24 × 0.199 × 0.097 |
| 2Θ range for data collection/° | 4.022 to 61.348 |
| Index ranges | $-27 \leq h \leq 27, -10 \leq k \leq 10, -29 \leq l \leq 29$ |
| Reflections collected | 34428 |
| Independent reflections | 4388 [R$_{int}$ = 0.0367, R$_{sigma}$ = 0.0206] |
| Data/restraints/parameters | 4388/20/258 |
| Goodness-of-fit on F$^2$ | 1.061 |
| Final R indexes [I>=2σ (I)] | R$_1$ = 0.0164, wR$_2$ = 0.0373 |
| Final R indexes [all data] | R$_1$ = 0.0183, wR$_2$ = 0.0380 |
| Largest diff. peak/hole/e Å$^{-3}$ | 0.46/−0.37 |
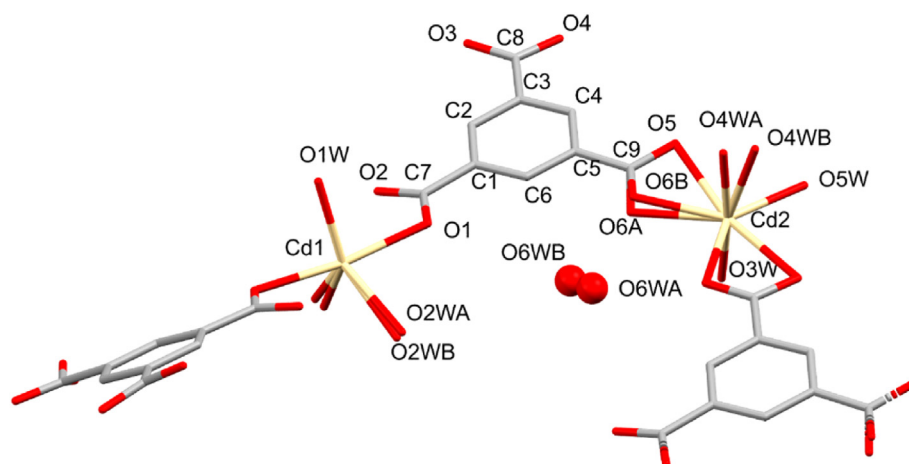
**Figure 1.** Coordination spheres of the two unique cadmium ions in **CP1**. Only ASU atoms are labelled and hydrogen atoms are omitted for clarity.
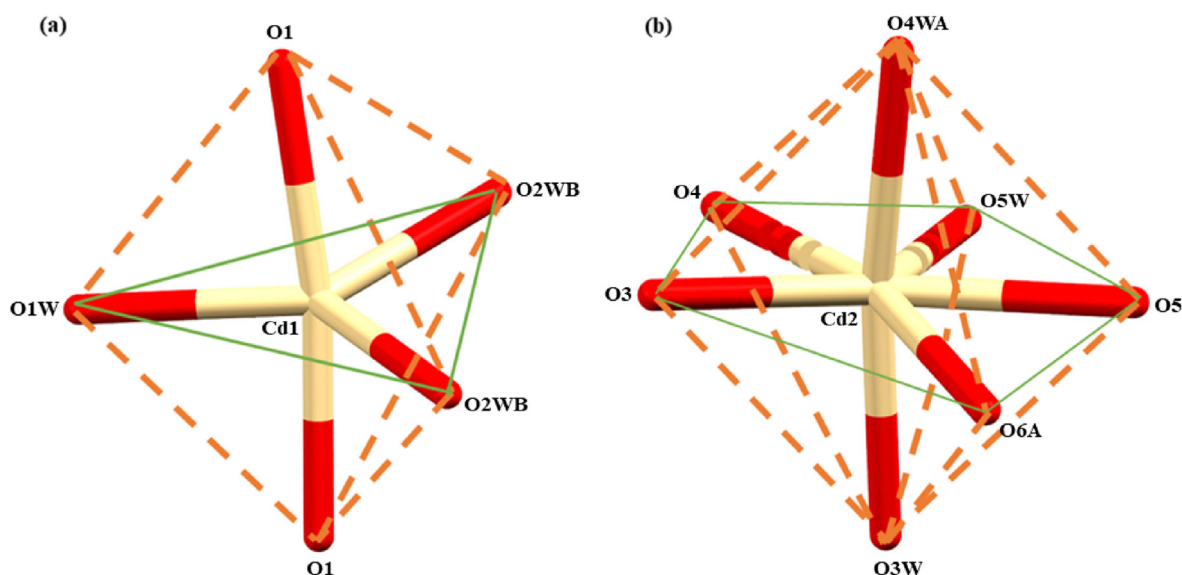


**Figure 2.** Coordination geometry around the Cd1 and Cd2 ions in **CP1**. Only the major components of disordered positions are shown (labelled A or B).

proceeding using the full-matrix least square method, based on $F^2$ values against all reflections, including anisotropic displacement parameters for all non-H atoms, as employed in SHELXL-2018/3 [12,13]. X-Seed and MERCURY were used for generating high-quality images using POV-RAY [8,14,15]. PLATON was used to identify intermolecular hydrogen-bonding interactions [16].

## 3. Results and discussion

Single crystal X-ray diffraction analysis revealed that **CP1** crystallizes in the monoclinic crystal system in the space group *C2/c* (Table 1). The asymmetric unit (ASU) comprises of one and a half cadmium(II) ions, one fully deprotonated, bridging benzene-1,3,5-tricarboxylate (BTC) anion, four and a half coordinated water molecules and one uncoordinated water molecule (Figure 1). The total 3+ charge on the one and half crystallographically unique $Cd^{2+}$ ions is counter-balanced by the 3-charge of the fully deprotonated BTC ligand. Cd1 is located on a 2-fold axis and has a distorted trigonal bipyramidal coordination environment with coordination bonds that range from 2.251 to 2.296 Å, which agree

well with the reported structures at 293 K (Figure 2a). The two axial positions are occupied by the O1 and O1_i (i: 1 − x, y, 3/2 − z) atoms of two different BTC anions (related by a 2-fold axis) that bind in a mono-dentate fashion, whilst three water molecules, O1W, O2W and O2W_i occupy the equatorial positions. Furthermore, O2W is disordered over two positions with site occupancy factors (sofs) of 0.44 and 0.56 for the A and B labelled positions, respectively (Figure 1). Cd2 has a pentagonal bipyramidal coordination environment; the axial positions being occupied by oxygen atoms of two water molecules (O3W and O4W), whilst the equatorial positions are occupied by O5W of a water molecule, two oxygen atoms (O5 and O6) from one carboxylate group of a BTC anion and two oxygen atoms O3_ii and O4_ii (ii: −½ + x, −½ + y, z) from the carboxylate group of a second BTC anion (Figure 2b). All the carboxylate groups are bonded to the Cd2 metal centres in bidentate coordination mode. In addition, the coordinated O4W water molecule is disordered over two positions with sofs of 0.77 and 0.23, for the A and B-labelled positions, respectively (Figure 1). The uncoordinated water molecule (O6W) is also disordered over two positions with sofs of 0.66 and 0.34, for the A and B-labelled positions, respectively (Figure 1). The reported
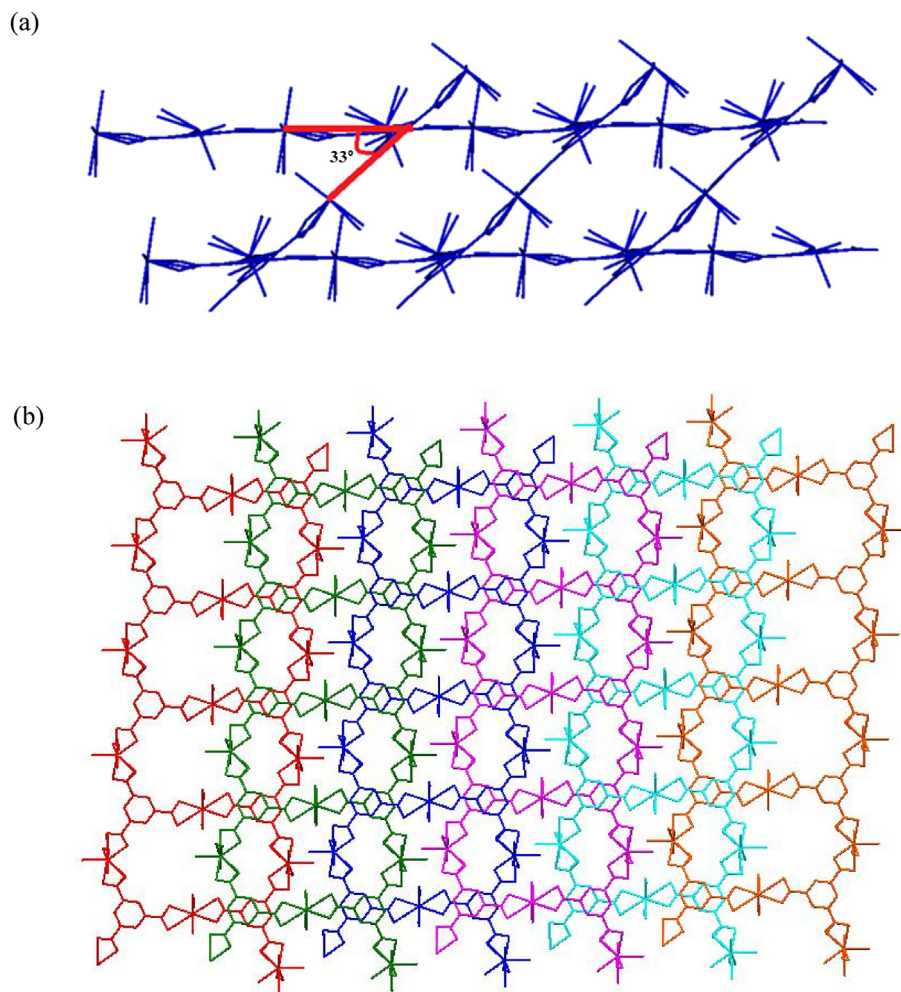
(a)



(b)



**Figure 3.** Views along (a) the *c*-axis (oblique view of the *ab* plane) showing two co-planar directions of the bidentate coordination with an angle of 33° and (b) the *b*-axis (directly onto the *ac* plane) showing the interdigitation of neigbouring 2-periodic frameworks (each framework is colour coded). Hydrogen atoms have been omitted for clarity.

structures at 293 K showed no signs of disorder for any of the atoms, except for uncoordinated water molecules, as indicated in the structure of Wu et al. [7].

**CP1** is a coordination polymer where the coordination is extended infinitely in two co-planar directions by the bidentate coordination of two carboxylate groups (O3 and O4; O5 and O6) of the BTC anions to Cd2 ions. These co-planar 1D 'strands' make an angle of 33° with each other (Figure 3a). In turn these strands are connected via finite monodentate coordination of the third carboxylate group (O6) of the BTC anions to the

Cd1 ions. The combination of the coordination modes results in 2-periodic frameworks that extend infinitely in the *ab* plane, whilst being interdigitated with each other along the *c*-axis direction (Figure 3b).

Intermolecular hydrogen bond analysis reveals that the water molecules are involved in several hydrogen bonds, with mostly coordinated water molecules acting as hydrogen bond donors to carboxylate oxygen acceptor atoms (Table 2). These hydrogen bonds show that neighbouring 2D frameworks are connected to each other and thus that the coordinated water molecules play an integral role in the stability of the 3D structure

**Table 2.** Hydrogen bond geometry for **CP1** involving water molecules.

| D−H·····A | d(D−H)/Å | d(H···A)/Å | d(D···A)/Å | <D−H···A/° | Symmetry operation |
|---|---|---|---|---|---|
| O6WA-H6WA···O3 | 0.87 | 1.93 | 2.772 (3) | 164 | 1 − x,1 − y,1 − z |
| O3W–H3WA···O6WA | 0.87 | 1.69 | 2.718 (8) | 166 | x,y,z |
| O3W–H3WA···O6WB | 0.87 | 1.89 | 2.718 (2) | 159 | x,y,z |
| O3W–H3WB···O2 | 0.87 | 1.79 | 2.640 (2) | 166 | 1 − x,1 − y,1 − z |
| O5W–H5WA···O3W | 0.87 | 1.90 | 2.702 (2) | 153 | 1/2 − x,1/2 + y,1/2 − z |
| O5W–H5WB···O5 | 0.87 | 2.02 | 2.798 (2) | 147 | 1/2 − x,−1/2 + y,1/2 − z |
| O1W–H1WA···O4 | 0.87 | 1.93 | 2.752 (1) | 156 | 1 − x,2 − y,1 − z |
| O1W–H1WB···O4 | 0.87 | 1.91 | 2.752 (1) | 163 | x,2 − y,1/2 + z |
| O4WA–H4WA···O1 | 0.87 | 1.80 | 2.655 (2) | 165 | 1/2 − x,3/2 − y,1 − z |
| O2WB–H2WA···O4 | 0.87 | 1.89 | 2.71 (2) | 155 | 1 − x,1 − y,1 − z |
| O2WB–H2WB···O5 | 0.87 | 1.84 | 2.69 (2) | 166 | x,1 − y,1/2 + z |
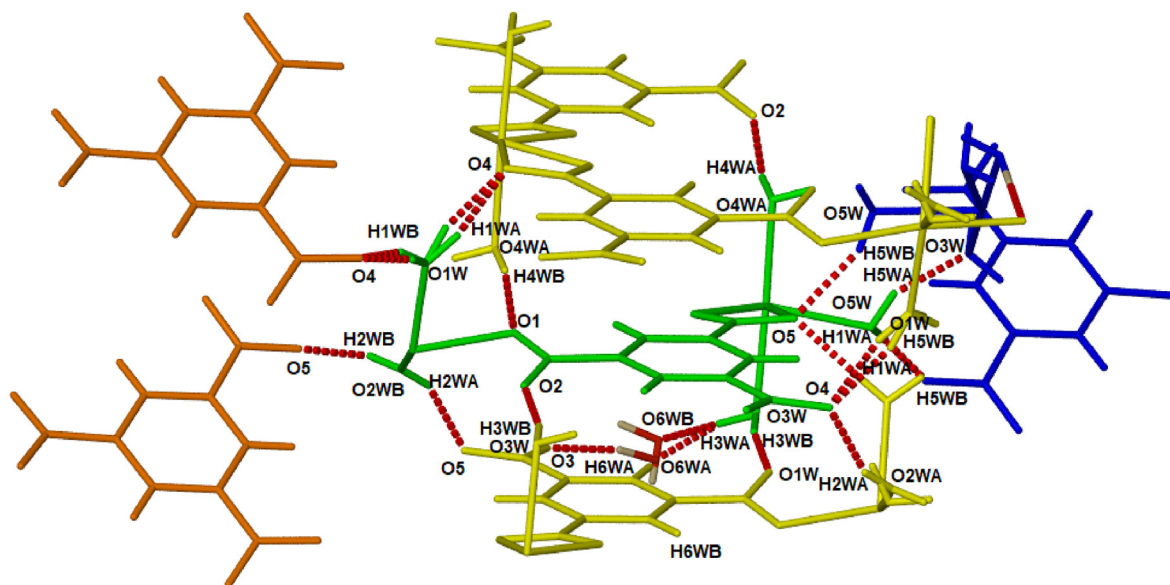
**Figure 4.** Hydrogen bonding in **CP1** between the ASU (shown in green) and surrounding atoms. Colour-coded moieties belong to the same 2-periodic framework.
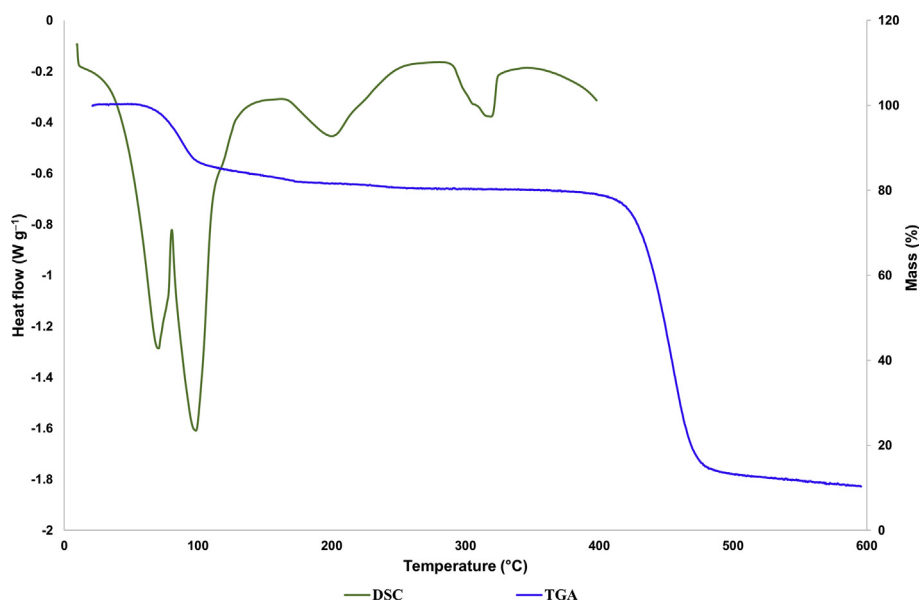


**Figure 5.** Overlay of DSC (**green**) and TGA (**blue**) thermograms of **CP1**.

(Figure 4). In addition, the uncoordinated water molecule (O6WA position) acts as an indirect link between two neighbouring frameworks by acting as both a hydrogen bond donor (O6WA-H6WA⋯O3) and acceptor (O3W–H3WA⋯O6WA).

### 3.1. Thermal analysis

The TGA thermogram of **CP1** indicates a two-step mass loss event, comprising of initial solvent loss around ~50 °C, which significantly increases thereafter. The total mass loss occurring in the range of 50–400 °C is found to be 21.2 % (Calc. 20.85 %), fully accounting for the 5.5 water molecules per ASU. The DSC thermogram showed two overlapping endotherms between 50-100 °C, which probably corresponds to the concomitant release of uncoordinated and coordinated water molecules from the framework. Two other endothermic bands appear around 185

°C and 305 °C, which probably correspond to additional solvent loss as indicated by TGA (Figure 5). The framework decomposed after 400 °C.

A clear effect of dehydration can be vizualized from HSM analysis where crystals of **CP1** were placed under silicone oil and heated in a range of 25–450 °C (Figure 6). Although the first sign of solvent loss was noticed around 80 °C, the bubbles evidently came off at 120 °C (Figure 6). The clear crystal started to turn opaque at this stage, which at the very least indicates the loss of monocrystallinity due to loss of solvent molecules. Around 400 °C they became brown indicating decomposition of the framework.

### 3.2. Powder X-ray diffraction studies

The PXRD pattern of compound **CP1** recorded at room temperature and ambient pressure is in good agreement with its calculated pattern which proves the phase purity of the bulk material (Figure 7).
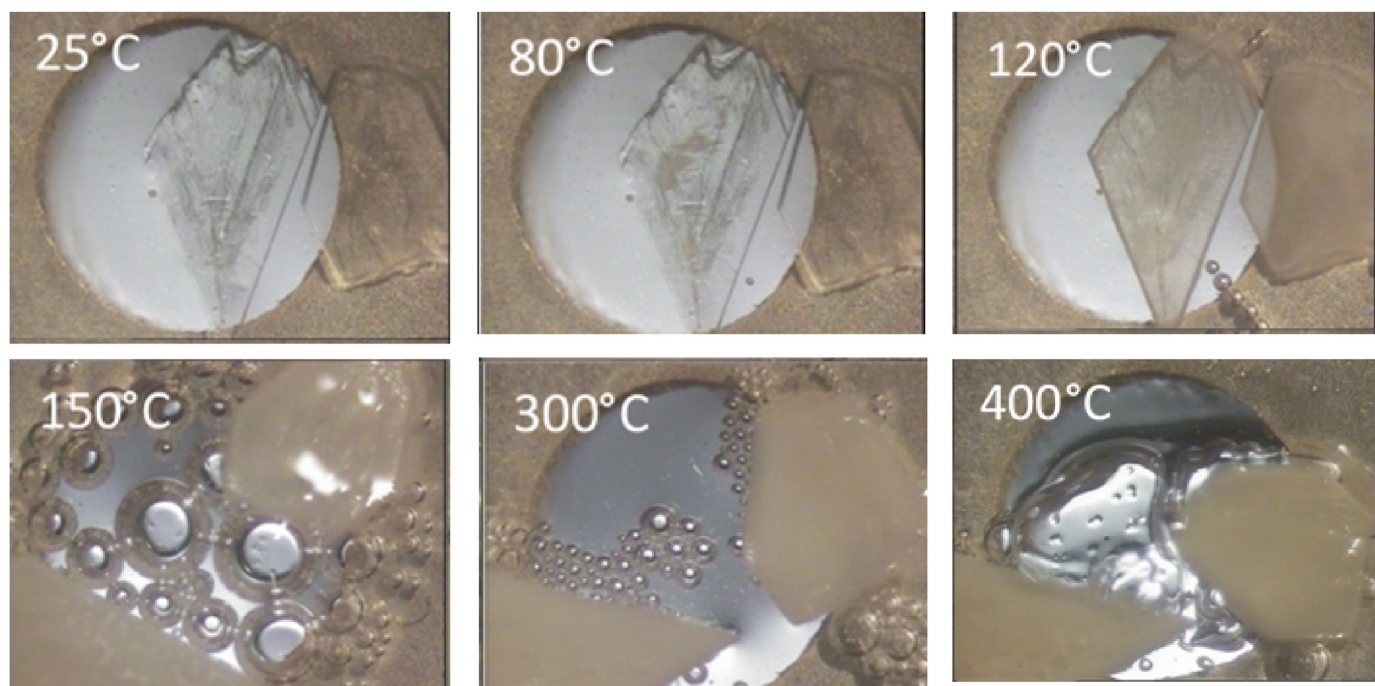
**Figure 6.** Hot stage microscope photographs of compound **CP1** under silicone oil at various temperatures (bubbles indicate the release of solvent).
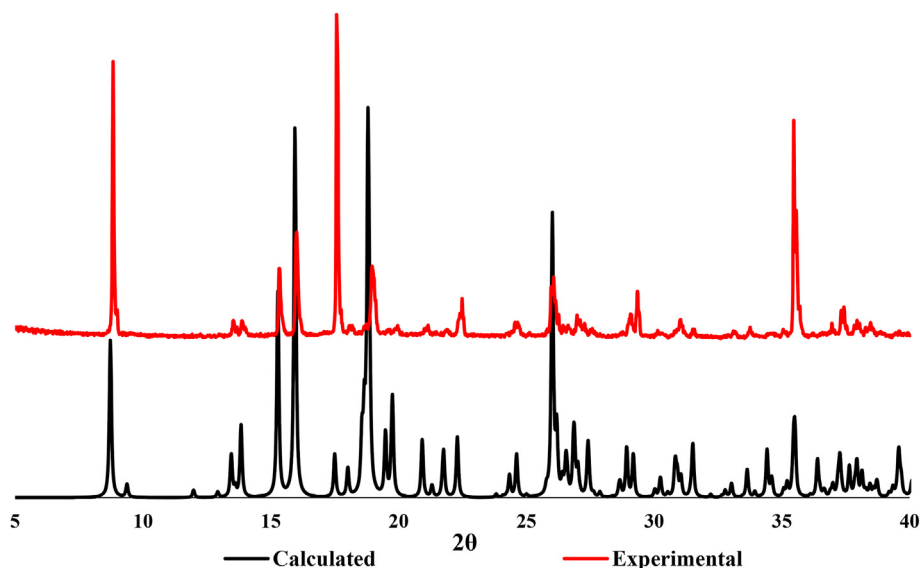


**Figure 7.** Comparison of the experimental PXRD pattern of **CP1** with the calculated PXRD pattern obtained from the single crystal structure.

### 3.3. Dehydration and rehydration studies

These studies were performed to investigate whether the dehydrated sample of **CP1** (hereinafter **CP1′**) is able to transform to the original structure of **CP1** by readsorbing moisture from the atmosphere (hereinafter **CP1′R**). TGA and PXRD experiments were used in conjunction to assess whether structural changes occurred when **CP1** is dehydrated and rehydrated. A TGA thermogram of a fresh sample of **CP1** was recorded first by heating the sample to 200 °C (Figure 8a). The sample was then cooled and immediately reheated (no exposure to air), after which no mass loss occurred on the reheating, confirming that all the solvent was released in the first run. This same sample was then exposed to water vapour by placing it in a smaller vial that was placed in a bigger vial with water. After two days, the TGA analysis revealed that the original amount of water was readsorbed. The corresponding PXRD patterns of the samples at different stages of the experiment show not only that the original amount of water is readsorbed but that the structure of **CP1′R** corresponds to the structure of **CP1**, thus showing that the dehydration is reversible in terms of both the loss of water and crystallinity of **CP1** (Figure 8b).

*In situ* PXRD rehydration studies were also performed by using a modified sample stage which consisted of water wells next to the sample.
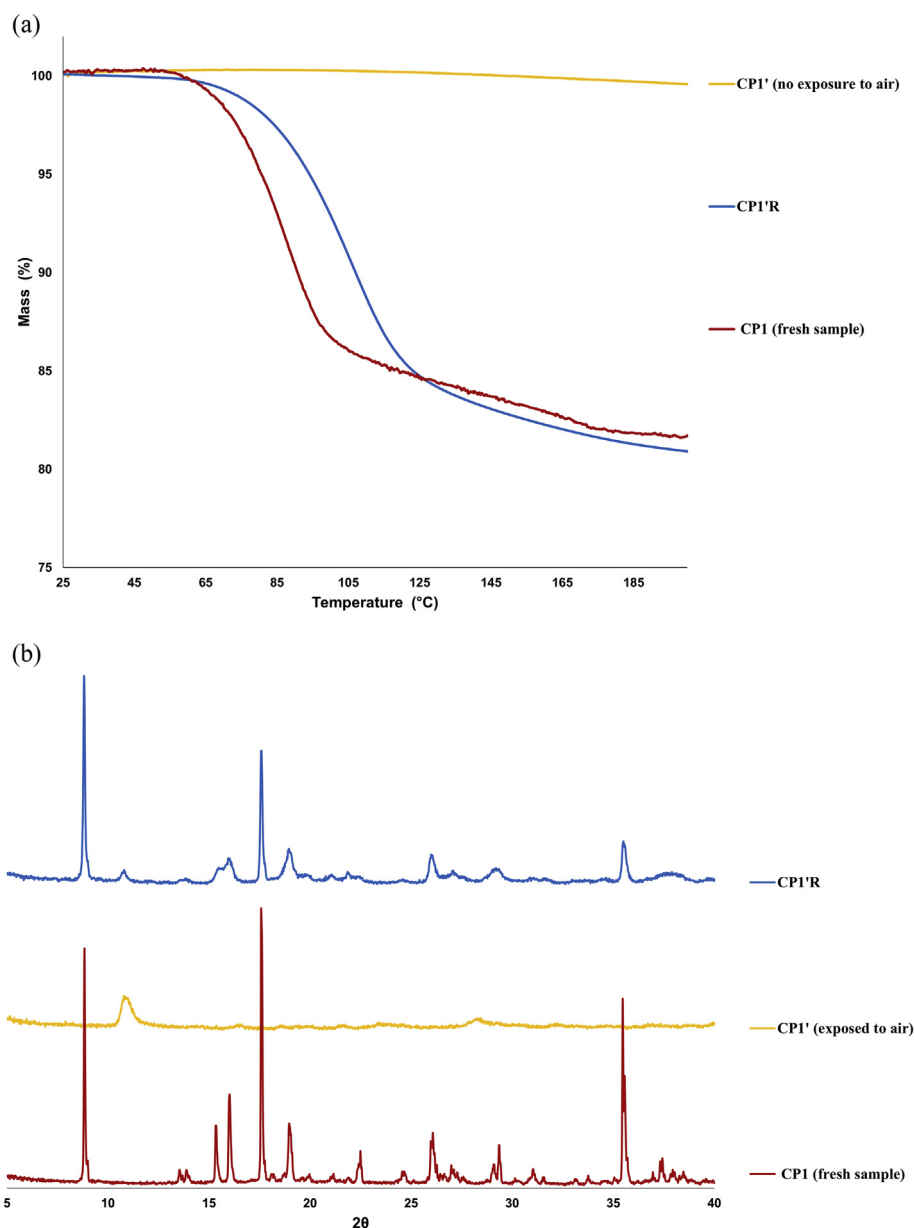
**Figure 8.** (a) TGA and (b) associated PXRD patterns of **CP1**, **CP1′** and **CP1′R**.

The sample was heated to 300 °C (maintained for 30 min) and cooled back to room temperature (~25 °C) before commencement of the *in situ* experiment. Diffractograms were recorded over a period of 14 h but after 3 h and 15 min no further changes in the patterns were observed. Each diffractograms was recorded over ~15 min in the scan range of 4–40° 2θ (Figure 9). Initially, the PXRD pattern indicates that the sample is amorphous but even after 15 min the sample regains crystallinity. Eventually after ~3 h the PXRD pattern matched that of the as-synthesized **CP1** sample (Figures 9 and 10).

### 3.4. Infrared spectroscopy

The infrared spectroscopy data further supports the reversibility of the dehydration of **CP1** when **CP1′** adsorbs moisture from the atmosphere. The IR spectrum of **CP1** (Figure 11) showed a broad band at the region of 3322–3096 cm$^{-1}$ that can be assigned to the asymmetric and symmetric OH streching vibration modes of water molecules [17, 18, 19]. This band was not observed in the IR spectrum of **CP1′** indicating the absence of the water molecules in the cavity. The presence of the metal coordinated water molecules in **CP1** was indicated by a strong band at 732 cm$^{-1}$ and was further proved by the shortening of that band upon dehydration in **CP1′** [20].

These bands do not completely disappear as the dehydrated sample readily absorbs moisture from air, which was proved by the TGA of the dehydrated sample exposed to moisture for 5 min only, which was the typical time required to perform the IR analysis (Figure 12). Those specific bands reappeared at the same position with same transmittance when **CP1′** was exposed to water vapour for two days.
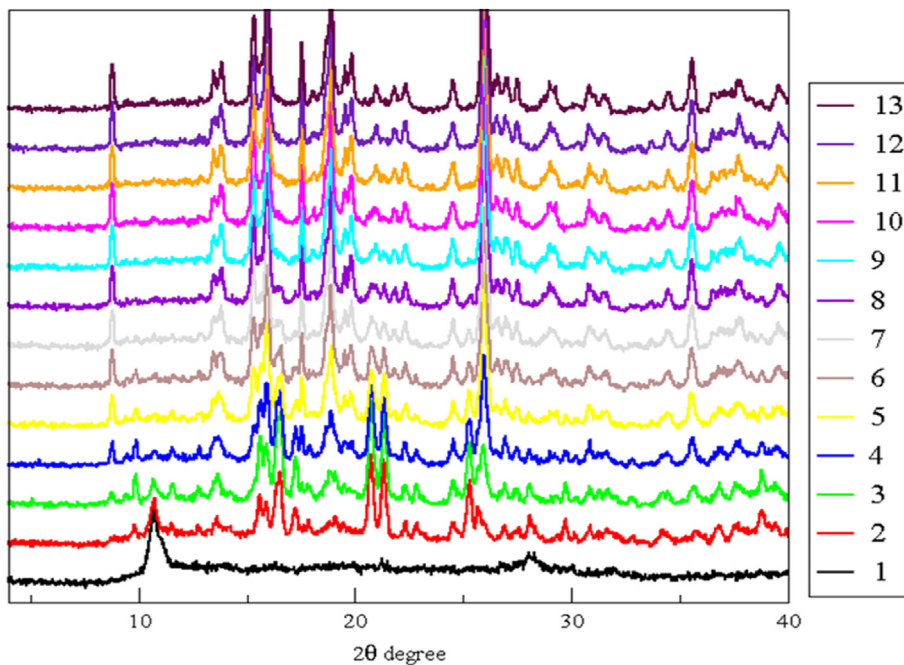
**Figure 9.** Evolution of PXRD diffractograms of **CP1**′ during water vapour exposure. Each step corresponds to 15 min. No patterns recorded after 3 h and 15 min are shown as those are similar to pattern 13.
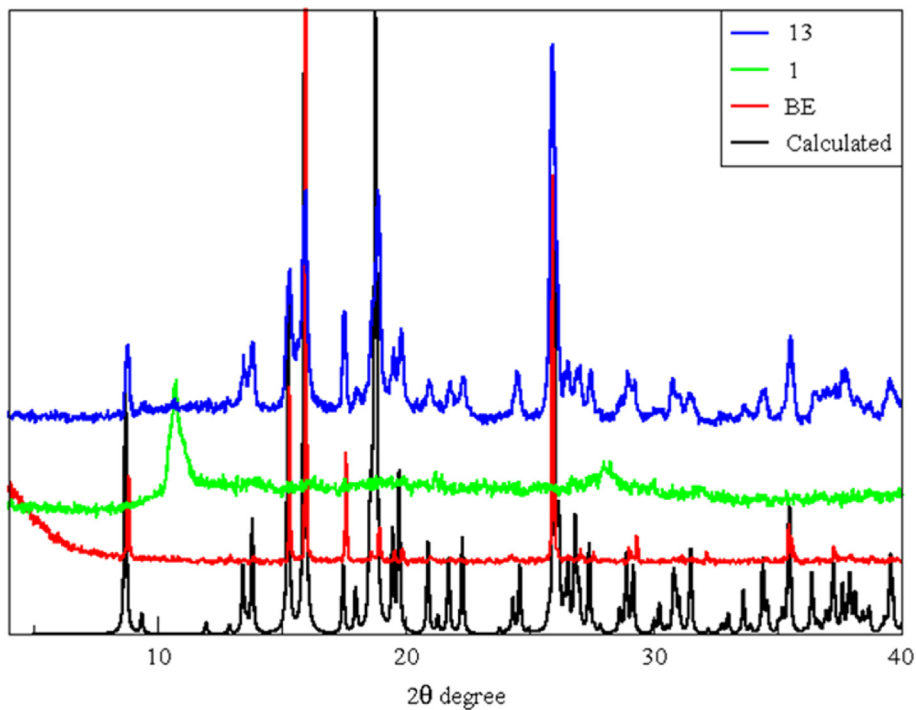


**Figure 10.** Comparison between different PXRD patterns of **CP1**, from bottom: calculated (black), recorded before *in situ* rehydration study (red) and the first (light green) and the last (blue) significant diffractograms recorded during the *in situ* experiment. BE = before experiment.
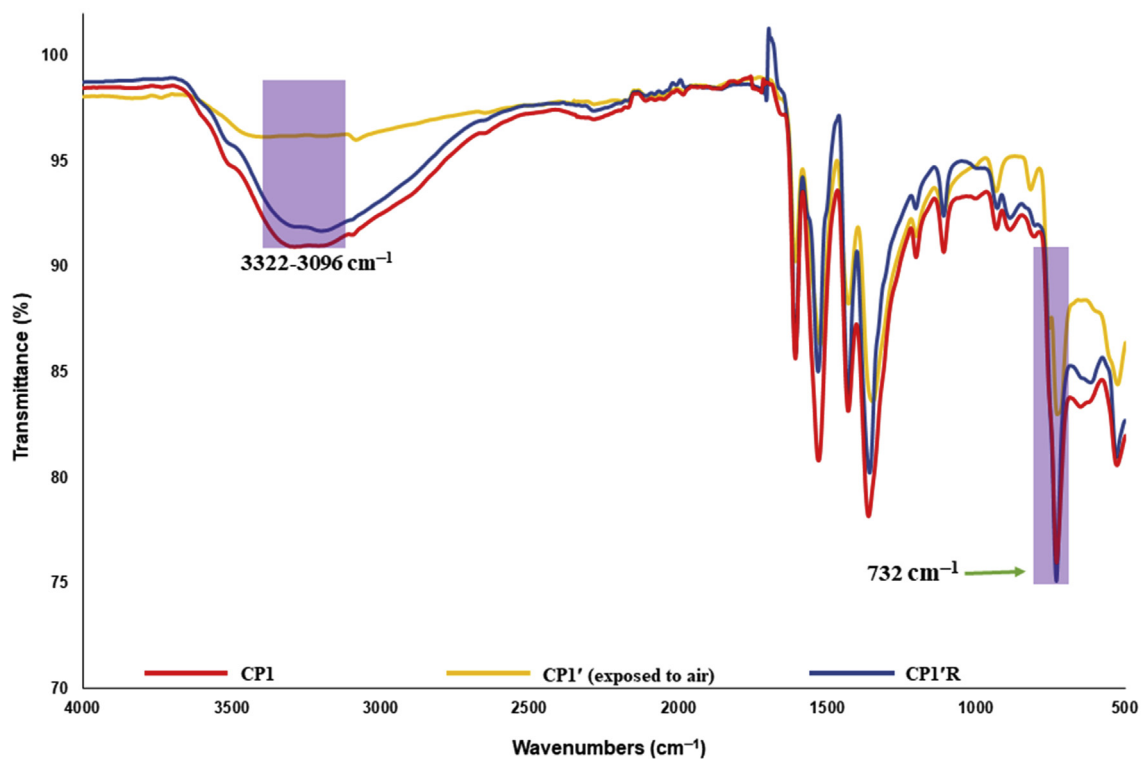
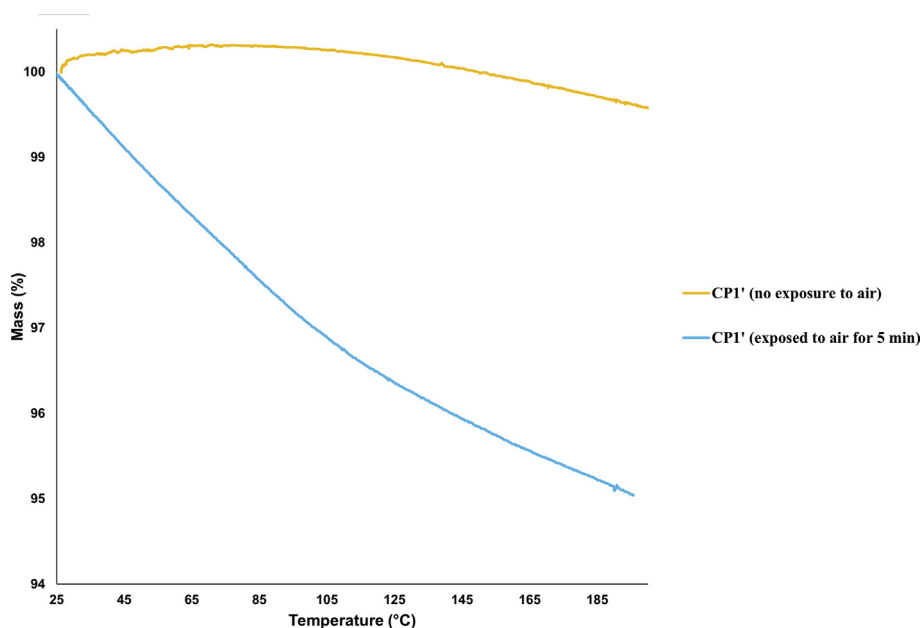**Figure 11.** IR spectra of **CP1**, **CP1′ (exposed to air)** and **CP1′R**.



**Figure 12.** TGA thermograms of **CP1′ not exposed to air** and exposed to air for 5 min.

## 4. Conclusion

In conclusion, a 2-periodic MOF has been resynthesized and subjected to single crystal X-ray diffraction reporting additional information on the hydrogen bonding present in the structure, as well as on the thermal properties, dehydration and rehydration behaviour, which were not reported in the previous studies on this compound. We have shown that this MOF can be rapidly rehydrated, after dehydration, upon exposure to water vapour which leads to regaining of the MOFs original structure.

Thus, it could prove useful as water scavenger in applications where dry environments are desired.

## Declarations

### Author contribution statement

Nabanita Chatterjee, Marcello Mutti: Performed the experiments; Analyzed and interpreted the data; Wrote the paper.

Paolo Pelagatti: Analyzed and interpreted the data; Wrote the paper.

Clive L. Oliver: Conceived and designed the experiments; Analyzed and interpreted the data; Contributed reagents, materials, analysis tools or data; Wrote the paper.

## Data availability statement

Data associated with this study has been deposited at Cambridge Crystallographic Data Centre.

## Declaration of interests statement

The authors declare no conflict of interest.

## Additional information

Supplementary content related to this article has been published online at https://doi.org/10.1016/j.heliyon.2022.e10299.

## References

[1] C. Guo, F. Duan, S. Zhang, L. He, M. Wang, J. Chen, J. Zhang, Q. Jia, Z. Zhang, M. Du, Heterostructured hybrids of metal–organic frameworks (MOFs) and covalent–organic frameworks (COFs), J. Mater. Chem. 10 (2022) 475–507.

[2] L.E. Kreno, K. Leong, O.K. Farha, M. Allendorf, R.P. Van Duyne, J.T. Hupp, Metal–organic framework materials as chemical sensors, Chem. Rev. 112 2 (2012) 1105–1125.

[3] M. Gupta, N. Chatterjee, D. De, R. Saha, P.K. Chattaraj, C.L. Oliver, P.K. Bharadwaj, Metal−Organic frameworks of Cu(II) constructed from functionalized ligands for high capacity $H_2$ and $CO_2$ gas adsorption and catalytic studies, Inorg. Chem. 59 (2020) 1810–1822.

[4] H. Zhou, J.R. Long, O.M. Yaghi, Introduction to metal-organic frameworks, Chem. Rev. 112 (2012) 673–674.

[5] C. Wang, X. Liu, N.K. Demir, J.P. Chen, K. Li, Applications of water stable metal–organic frameworks, Chem. Soc. Rev. 45 (2016) 5107–5134.

[6] A. Dimos, A. Michaelides, S. Skoulika, A molecular bilayer motif constructed from a three-connected organic ligand and $Cd^{2+}$ cations: crystal structure of $[Cd_3(trimesate)_2(H_2O)_9].2H_2O$, Chem. Mater. 12 (2000) 3256–3258.

[7] J.-C. Dai, X.-T. Wu, Z.-Y. Fu, C.-P. Cui, S.-M. Hu, W.-X. Du, L.-M. Wu, H.-H. Zhang, R.-Q. Sun, Synthesis, structure, and fluorescence of the novel cadmium(II)-Trimesate coordination polymers with different coordination architectures, Inorg. Chem. 41 (2002) 1391–1396.

[8] C.F. Macrae, I. Sovago, S.J. Cottrell, P.T.A. Galek, P. McCabe, E. Pidcock, M. Platings, G.P. Shields, J.S. Stevens, M. Towler, P.A. Wood, Mercury 4.0: from visualization to analysis, design and prediction, J. Appl. Crystallogr. 53 (2020) 226–235.

[9] Bruker Apex3 v2019.3, SAINT V8.40A, Bruker AXS Inc., Madison, WI, USA, 2019.

[10] G.M. Sheldrick, SADABS, Version 2.05, University of Göttingen, Germany, 2007.

[11] O.V. Dolomanov, L.J. Bourhis, R.J. Gildea, J.A.K. Howard, H. Puschmann, OLEX2: a complete structure solution, refinement and analysis program (2009), J. Appl. Crystallogr. 42 (42) (2009) 339–341.

[12] G.M. Sheldrick, SHELXT - integrated space-group and crystal-structure determination, Acta Crystallogr. A: Found. Adv. 71 (2015) 3–8.

[13] G.M. Sheldrick, Crystal structure refinement with SHELXL, Acta Crystallogr. Section C-Struct. Chem. 71 (2015) 3–8.

[14] L.J. Barbour, X-Seed 4: updates to a program for small molecule supramolecular crystallography, J. Appl. Crystallogr. 53 (2020) 1141–1146.

[15] POV-Ray for Windows, Ver. 3.6, Persistence of Vision Raytracer, Pty. Ltd., 2004.

[16] A.L. Spek, Structure validation in chemical crystallography, Acta Crystallogr. Sect. D Biol. Crystallogr. 65 (2009) 148–155.

[17] S.C. Manna, S. Mistri, A.D. Jana, A rare supramolecular assembly involving ion pairs of coordination complexes with a host–guest relationship: synthesis, crystal structure, photoluminescence and thermal study, Cryst. Eng. Comm. 14 (2012) 7415–7422.

[18] M. Hakimi, K. Moeini, Z. Mardani, F. Mohr, Microwave-assisted template synthesis of diazacyclam-based macrocyclic copper complex and forming octahedral, square planar and square pyramidal geometries by ion exchanging and introducing a novel 2D square-grid copper–mercury coordination polymer, Polyhedron 70 (2014) 92–100.

[19] K. Nakamoto, Infrared and Raman Spectra of Inorganic and Coordination Compounds, Wiley, New York, 1986.

[20] J. Fujita, K. Nakamoto, M. Kobayashi, Infrared spectra of metallic complexes. II. The absorption bands of coordinated water in aquo complexes, J. Am. Chem. Soc. 78 (1956) 3963–3965.